

Article

Experimental Study on Activation Energy and Microstructure of Nano- and Micro-Sized Pozzolanic Materials as Cementitious Composite Binder

Won-Woo Kim * and Jae-Heum Moon

Structural Research Division, KICT (Korea Institute of Civil Engineering and Building Technology), Il-san, Goyang-si 10223, Gyeonggi-do, Republic of Korea

* Correspondence: kimwonwoo@kict.re.kr

Abstract: Silicate-based nano- and micro-sized binders were used with ordinary Portland cement to evaluate their influence on the setting time, activation energy, mechanical properties, and microstructure. It was found that the setting time was reduced due to the pozzolanic reaction of the silicate-based binders and the densification of the microstructure. However, there is a lack of research on nano-sized pozzolanic materials. Therefore, in this study, research on activation energy and microstructure was conducted. The compressive strength increased owing to a reduction in the porosity in the microstructure, and activation energy also tended to decrease. Moreover, using both micro-silica and a small proportion of nano-silica was more effective in reducing the setting time and activation energy than using any of them individually. The study established that adding a small proportion of nano-silica could reduce the setting time and increase the compressive strength because it positively influenced the pozzolanic reaction and filled the pores between micro-silica and cement, which were composed of relatively larger particles, with smaller particles. Because nanomaterials may degrade flowability due to their large specific surface area, it is deemed necessary to consider the addition of chemical admixtures during mix design. A characteristic has been revealed when nanomaterials are used, and special attention to the particle size distribution characteristics is required because the imbalance in particle size distribution may increase the porosity inside the microstructure. Therefore, it is recommended to use micro-sized pozzolanic materials together when using nano-sized pozzolanic materials.

Keywords: ultrahigh-performance concrete; advanced cementitious materials; cement reaction rate; reactive siliceous materials



Citation: Kim, W.-W.; Moon, J.-H. Experimental Study on Activation Energy and Microstructure of Nano- and Micro-Sized Pozzolanic Materials as Cementitious Composite Binder. *Buildings* **2023**, *13*, 3085. <https://doi.org/10.3390/buildings13123085>

Academic Editors: Binsheng (Ben) Zhang and Chuang Feng

Received: 4 October 2023
Revised: 27 November 2023
Accepted: 5 December 2023
Published: 12 December 2023



Copyright: © 2023 by the authors. Licensee MDPI, Basel, Switzerland. This article is an open access article distributed under the terms and conditions of the Creative Commons Attribution (CC BY) license (<https://creativecommons.org/licenses/by/4.0/>).

1. Introduction

Advancements in technology and development of various new materials have influenced paradigm shifts in the construction materials industry as well. This has resulted in the development of nano- and micro-sized pozzolanic materials for application as additives to cement [1]. Representative micro-sized pozzolanic materials that are used in ultra-high-performance concrete (UHPC) include pozzolanic binders and fillers, such as micro-silica and silica sand [2,3]. UHPC is a material whose compressive strength depends on the reactivity and particle size distribution optimization of the binders and fillers. Reactive siliceous materials enhance strength as binders because they cause the pozzolanic reaction and serve to increase the strength of concrete through the internal filling effect that fills the voids inside the cement composite with relatively finer particles, compared to cement [4,5]. A majority of the current studies on UHPC are primarily focused on the application of micro-sized pozzolanic materials and carbon-based nanomaterials [6–8], although there are a few applications of nano binders as well. For a material to be applied as a binder, research on its hydration reaction and activation is essential [9].

Maturity and activation energy are key factors for understanding the chemical reaction rate and degree of activation of cement [10]. Research on these factors is imperative to understand and optimize the reactivity and performance improvement of cement-containing nanomaterials. Mixing nanoparticles with conventional cement changes the properties of the composite materials and has the potential to positively influence the strength and durability of cement concrete. However, previous studies on cement-containing nanomaterials were mostly mechanical-performance-oriented experiments that failed to address the hydration reaction mechanism and activation energy of cement-containing nanomaterials [11–13].

Research on changes to the activation energy when nanomaterials are added to cement mixtures is necessary to decide on the application of new materials as cement binders. Such research can provide vital information on measurement of activation energy, control of reaction rate in relation to time and temperature, and interactions between nanomaterials and cement. Particularly, activation energy plays a key role in controlling the cement reaction rate because the cement reaction rate decreases as activation energy increases and vice versa [10,14]. Essentially, the curing rate as well as the strength and performance over time of cement-containing nanomaterials can be controlled by adjusting the reaction rate [15]. The outcome of such research is bound to provide new perspectives that would affect the applicability of nanomaterials in the field of construction materials and lead to technical advances for cement mixed with nanomaterials. The purpose of such research would be to perform experiments on the reactivity and activation energy of cement-containing nanomaterials to improve overall performance of cement-based materials.

Studies on existing nanomaterials have shown excellent results using nano-SiO₂, nano-TiO₂, nano-alumina, etc. [16–19]. In particular, a lot of research is being conducted on nano-SiO₂, accounting for 44% of research on nanomaterial application [20]. However, most research uses alkaline activators. In the case of research using existing nano- and micro-sized pozzolanic materials, there is a lack of research on their reactivity as a binder, and most of the research is simply on strength enhancement as a filler.

Therefore, in this study, the activation energy was measured and the microstructure was analyzed to determine the effect on the reactivity and microstructure of nano- and micro-SiO₂, which has reactivity without using an alkali activator.

2. Experimental Design and Methods

2.1. Experimental Materials and Mix Information

Ordinary Portland Cement (OPC) from company A in Korea was used in this study. Additionally, 15 nm nano-silica from company S and micro-silica from company E were selected as silicate-based binders. Tables 1 and 2 present the chemical compositions and physical properties of OPC and silicate-based nano- and micro-sized pozzolanic materials used. It can be observed that cement comprises 61.6% of CaO and 20.7% of SiO₂, and the major component in silicate-based nano- and micro-sized pozzolanic materials is SiO₂, whose content varies from 98.74 to 99.78%. The particles of silicate-based nano- and micro-sized pozzolanic materials vary approximately from 0.75% to 0.07% the particle size of cement. Their specific surface area varies approximately 47 to 612 times larger compared to cement as the particle size decreases. Table 3 shows the mix proportions of cementitious composites. The water-to-binder (W/B) ratio was kept constant at 0.3, whereas the types and ratio of binders were set as variables. Chemical admixtures, such as superplasticizers, were not used because they affect the setting times of the cementitious composites.

Table 1. Chemical composition of OPC.

	Chemical Composition (%)							
	LOI	SiO ₂	Al ₂ O ₃	Fe ₂ O ₃	CaO	MgO	SO ₃	K ₂ O
OPC	3.2	20.7	5.2	3.4	61.6	2.1	2.6	0.9

LOI: loss on ignition.

Table 2. Construction binder materials and nanomaterials [21].

Product Name	Ingredients	Size (nm)	Specific Surface Area (m ² /g)	Specific Gravity
OPC	CaO, SiO ₂ , Al ₂ O ₃ , Fe ₂ O ₃ , etc.	20,000	0.38	3.10
Micro-silica	96.08	20–30	20.8	2.11
Nano-silica	99.78	14.05	203.8	1.40

Table 3. Cement and nano–micro-silicate binder paste mixing table of volume proportions.

Specimens	W/B (%)	Binder Volume (%)		
		Cement	Micro-Silica	Nano-Silica
OPC		100	-	-
MS10	0.30	90	10	-
NS1		99.0	-	1
MS10NS1		89.0	10	1

OPC: Ordinary Portland Cement; MS: micro-silica; NS: nano-silica.

2.2. Mix Design

It is practically difficult to use nano- and micro-sized pozzolanic materials in mix design based on weight because they have very low specific gravity and a much higher specific surface area than commonly used binders for construction [21]. The volume stability (soundness) of silica-based mixes is very important [22,23]. Therefore, mix design was implemented by calculating the volume proportion using the volume calculation method presented by Kim et al. [21], as shown in Table 3. The specific gravity values in Table 2 were used for conversion of weight to volume. Micro-silica is generally substituted up to 7 to 10% of cement in high-strength concrete mix [6–8,21]. Hence, in this case, 7.5% by weight of cement, which is approximately 10% when converted to volume proportion, was substituted with micro-silica. In the case of nano-silica, which has relatively small particle size, low specific gravity, and large specific surface area, a maximum content of 0.5 to 1% is recommended [12,21]. To examine the setting time when both micro-silica and nano-silica are added together, an additional experiment was performed on the mixture prepared with 10% micro-silica and 1% nano-silica. The cementitious composites were prepared using a paddle mixer in accordance with ASTM C 305 [24] and KS L 5109 [25], and the silicate-based nano- and micro-sized pozzolanic materials were subjected to dry mixing with cement. After dry mixing of cement and nano- and micro-sized pozzolanic materials was performed for 15 s, mixing water was added and mixing was performed at low speed (140 ± 5 r/min) for 30 s. Afterwards, after a rest period of mixing for about 30 s, mixing was carried out at medium speed (285 ± 10 r/min) for 1 min.

3. Experimental Method

3.1. Flowability (Flow Table) Measurement

Flowability of the cement pastes containing the silicate-based nano- and micro-sized pozzolanic materials was tested using a flow table (KS L 5111 [26]). In the test, the flow after 25 strikes was measured using a vernier caliper on the flow table. Measurements were performed twice for the same mix and the average value was used.

3.2. Setting Time (Vicat) Measurement

The setting time of cement paste was measured by the Vicat needle test method in accordance with ASTM C 191 [27], where CONTROLS's (Milan, Italy) Vicamatic2 automatic measurement system was used (Figure 1). To measure the initial and final setting times for each cement mix, the penetration depth was measured every 30 min after the start of the test. Because the penetration depth rapidly decreases closer to the initial setting time, the

penetrating needle was set to drop automatically every five minutes when the penetration depth became less than 30 mm. The initial reading of penetration depth was 38 mm. Due to the nature of the equipment and difficulties in obtaining measurements up to 0 mm, the final setting time was determined as the time when the penetration depth became less than 3 mm. Measurements were performed after stabilizing the cement paste for 24 h in a constant temperature and humidity chamber at curing temperatures of 10, 20, and 45 °C and humidity of 85%.



Figure 1. Automatic Vicat equipment.

3.3. Compressive Strength Measurement

The compressive strength of cement paste was measured to calculate the activation energy and verify the mechanical properties related to the addition of nano- and micro-sized pozzolanic materials. Cubic specimens of 50 mm were prepared to measure the compressive strength of the cementitious composites (Figure 2). The test specimens were subjected to water curing temperatures of 10, 20, and 45 °C and humidity of 85% in accordance with the procedure, and the compressive strength was measured at 2, 4, 8, 16, 32, and 64 times the final setting time determined through tests described in Section 3.2. The compressive strength was measured using a 300 kN universal testing machine (AG-300KMX of SHIMADZU, Kyoto, Japan) in accordance with ASTM C 109 [28]. Compressive strength was measured under a loading rate of 0.3 MPa/sec and the average value was presented for 6 specimens in each case.

3.4. Activation Energy Calculation

Calculating the activation energy helps analyze the correlation between improvement in the compressive strength and reactivity of the nanomaterials by obtaining the rate constant coefficient (k_t) based on ASTM C 1074 (2021) [29]. The rate constant coefficient can be obtained through linear regression analysis on the reciprocal of the strength measured

at multiples of the final setting time, which was determined from the cement setting time measurement test, and the reciprocal of the age. The value obtained by dividing the y -intercept of the linear equation, which is the result of the regression analysis, by the slope is the rate constant coefficient (Figure 3a). For example, based on OPC 20 °C in Figure 3a, the value obtained by dividing the y -intercept of the equation $y = 0.0186x + 0.013$, i.e., 0.013, by its slope, i.e., 0.0186, is the rate constant coefficient k_t . In this case, it is calculated to be 0.6989. Activation energy (E_a) can be measured from the results of the regression analysis on the natural log value of the rate constant coefficient and the reciprocal of the absolute temperature. As shown in Figure 3b, activation energy was calculated by multiplying the absolute value of the slope of the linear equation, which is the result of the linear regression analysis, by the gas constant (8.314 J/mol·K).



Figure 2. Production of specimens.

3.5. Microstructure (Nano-CT) Measurement

The microstructure of cement affects the durability and strength of concrete. Porosity of cementitious materials can be measured in various ways using the Brunauer–Emmett–Teller (BET) method, mercury intrusion porosimetry (MIP), and X-ray computed tomography (CT). BET, a method proposed by Brunauer, Emmett, and Teller, determines porosity inside the cement hydrate microstructure based on the amount of gas or water vapor adsorbed based on the gas adsorption theory. MIP is used to measure the amount of micropores and pore size distribution in the microstructure inside cement paste as with BET. It measures the internal porosity by injecting mercury. BET may be favorable for measuring micropores in a specific range, but the range of measurements is limited and pores larger than a certain size cannot be measured. For the purpose of this study, the influence of connected capillary pores bigger than 100 nm in size were considered to be within the main scope. Therefore, X-ray CT was selected for microstructure measurement even though the minimum size of pores to be observed was relatively large. It is a well-known fact with regard to cement concrete that connected capillary pores 100 nm or larger significantly affect their external deterioration and strength, whereas pores lower than 100 nm are most likely discontinuous and remain unconnected [28,29]. The X-ray CT measure equipment used was vltomelx m

microfocus CT of GE Sensing & Inspection Technologies (Boston, MA, USA). Specimens for measuring the porosity inside the microstructure using X-ray CT were prepared by precisely cutting the same specimens that were used for compressive strength measurement. Initially, they were subjected to water curing, precisely cut at the ages of 1, 7, and 28 days, and immersed in acetone to stop hydration before capturing images.

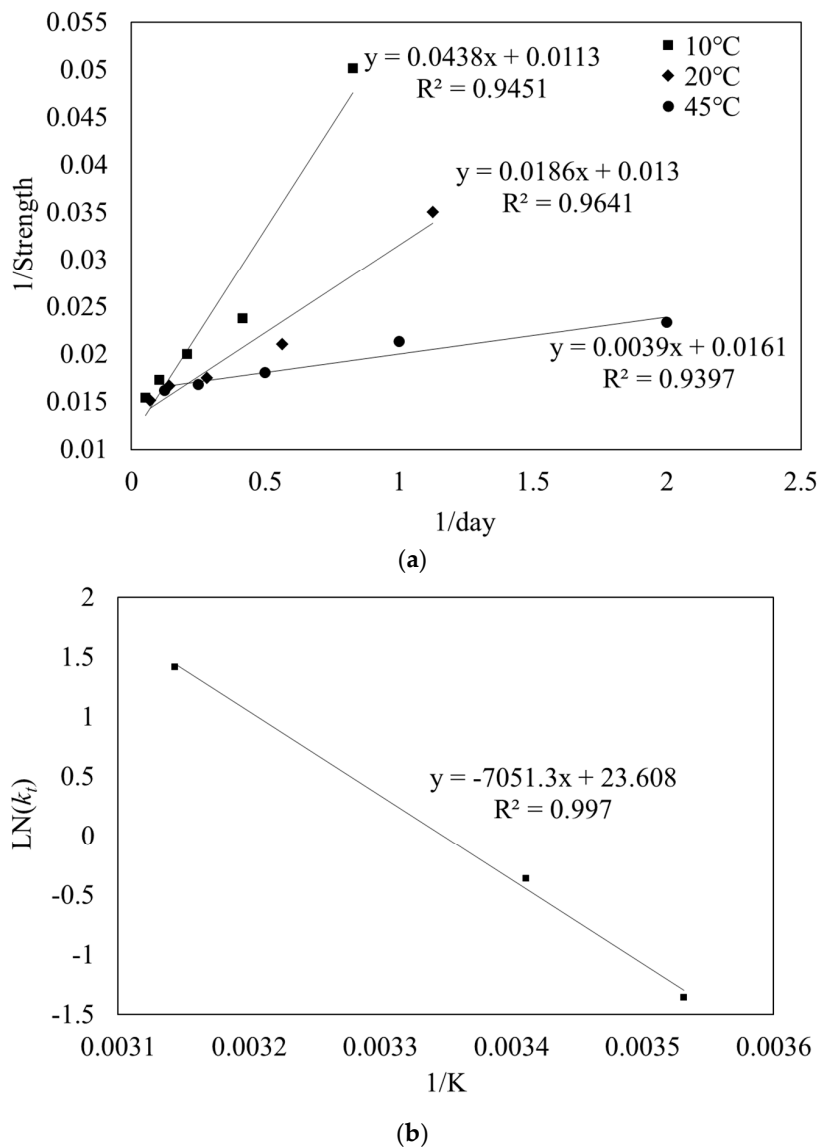


Figure 3. Activation energy determination method of cement paste. (a) Compressive strengths of cement pastes under different curing temperatures. (b) Determination of E_a using ASTM C 1074 [29].

4. Experiment Results and Discussion

4.1. Flowability

Figure 4 shows the flowability of the various cement pastes. Corresponding to the contents of pozzolanic binders, the flowability of all the mixes except that with silica fume showed a tendency to decrease. Cement paste prepared with only OPC, i.e., without any additives, exhibited the highest flowability (approximately 194 mm) followed by the paste containing micro-silica mix (183 mm) and nano-silica mix (158 mm). It appears that nano-silica significantly reduced flowability of the cement paste owing to comparatively lower density and higher specific surface area, although its content is approximately 1/10 of the contents of the other pozzolanic binders only, based on the volume.

Flowability of the mix containing both nano-silica and micro-silica was found to be 164 mm, which is higher than that of the mix containing only nano-silica. This appears to have been caused by the particle imbalance in the material, i.e., the large difference in the particle size between nano-silica and cement. However, the addition of micro-silica countered the negative effects of the imbalance in particle size and restored flowability to a certain extent. Therefore, to prevent reduction in flowability when nano-silica is added as a binder, it is necessary to consider countermeasures such as the addition of chemical admixtures to maintain particle size balance.

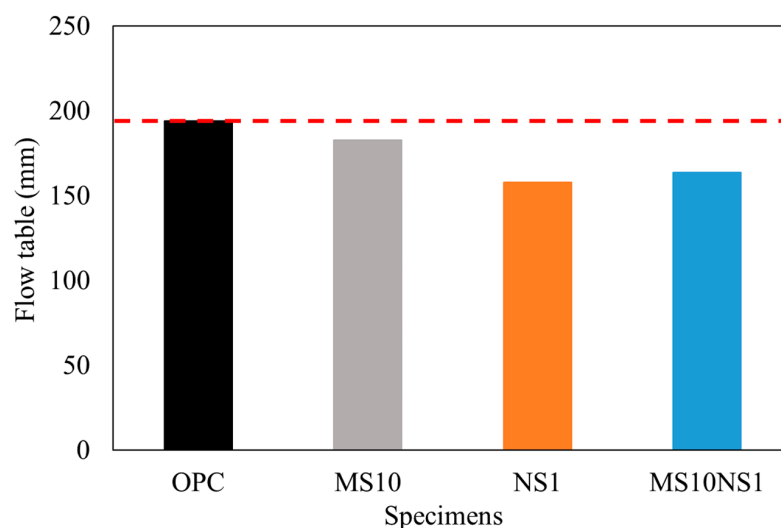


Figure 4. Flow table of silicate-based binder composites.

4.2. Setting Time Measurement Results

The setting time measurement results, in terms of the penetration depth over time corresponding to the various cement mixes with the addition of nano- and micro-sized pozzolanic materials, are presented in Figure 5. For measuring the initial and final setting time, curing of the specimens was conducted at 10, 20, and 45 °C temperature. The measurement results are grouped according to the curing temperatures, and the results of each temperature group are compared and discussed hereunder.

When cured at a temperature of 20 °C, the initial and final setting time for the OPC mix were measured to be 255 and 320 min, respectively. In the case of other mixes, the initial and final setting time tended to decrease, in comparison to OPC, depending on the silicate-based binder. For the micro-silica mix, the initial and final setting time were measured to be 152 and 190 min, respectively. Evidently, the nano-silica mix exhibited a setting acceleration effect due to the relatively lower content by recording initial and final setting time of 193 and 230 min, respectively. This indicates that nano-silica hydrated rapidly at the beginning by accelerating the pozzolanic reaction owing to the smaller particles and large specific surface area compared to the relatively low content. To analyze the effect of the particle size distribution, nano-silica whose specific surface area is approximately 10 times that of micro-silica was added together with micro-silica for a comparison. It was found that adding 1% of nano-silica reduced both the initial and final setting time. The initial and final setting times in this case were approximately 135 and 190 min, respectively. The final setting time was reduced by approximately 130 min compared to OPC. On the basis of the aforementioned observations, it can be stated that adding a small amount of nano-silica has the positive effect of reducing the setting time. In the mix that contained both micro-silica and nano-silica, it is apparent that nano-silica, with an average particle size of approximately 14.05 nm, together with micro-silica, with particle sizes of 20 to 30 nm, has dispersed evenly among cement, whose particle size is approximately 20,000 nm, and effectively reduced the setting times by serving as catalysts that accelerated hydration while simultaneously filling the voids in the microstructure.

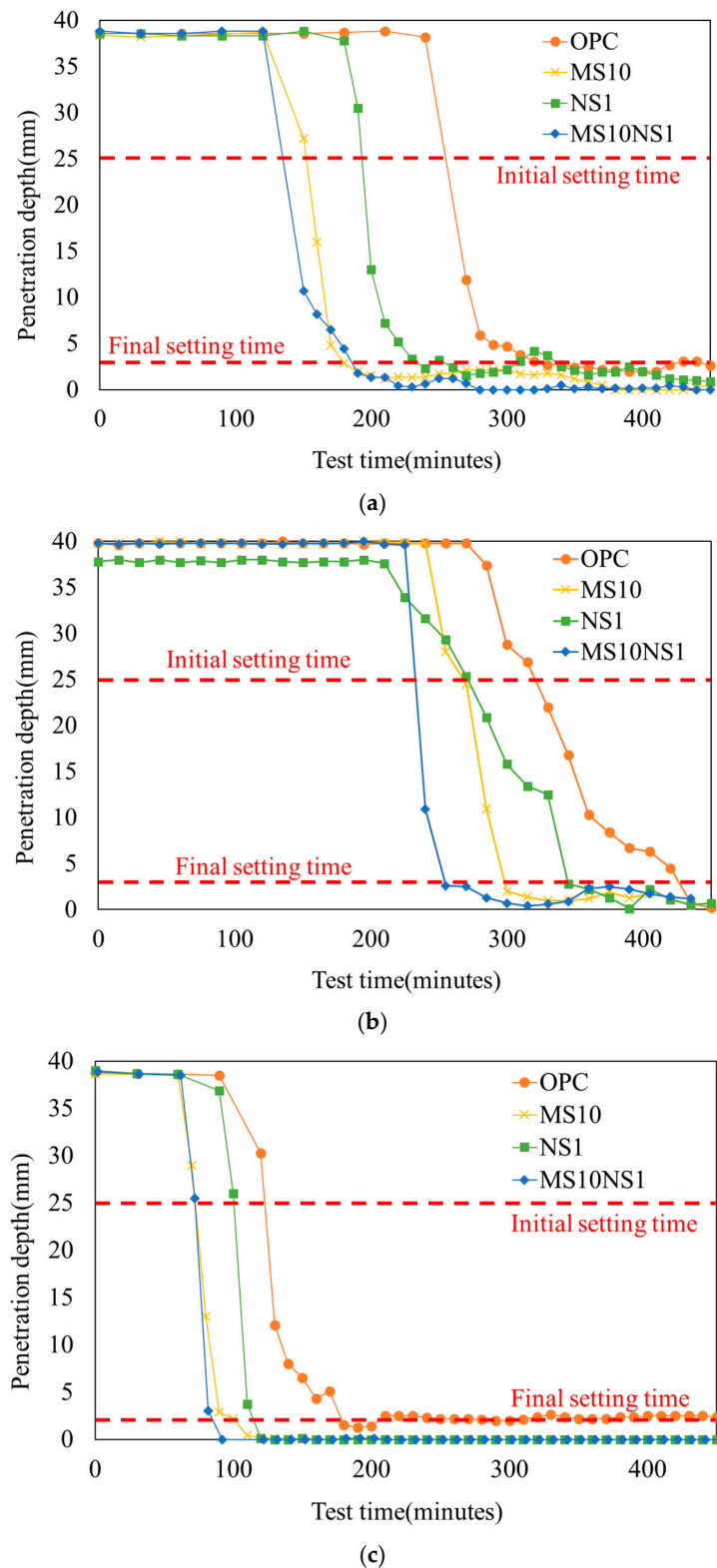


Figure 5. Vicat test result of silicate-based binder composites at curing temperatures. (a) 20 °C. (b) 10 °C. (c) 45 °C.

When cured at a temperature of 10 °C, the setting times were generally prolonged. The increase in setting time was more significant in the mixes that used the pozzolanic materials in comparison to OPC. Particularly, the mix that contained micro-silica exhibited the highest extension. However, in the mix that used both nano- and micro-silica, the

extension in setting time was reduced compared to the mixes in which the materials were used separately. Evidently, this could be because the silicate-based materials with relatively small particle size densely filled internal pores and generated hydrates inside the cement hydrate structure through the pozzolanic reaction, resulting in composite effects. Such effects are not significant when the nano-silicate-based materials were used alone, probably because of the large particle size difference, but use of both nano- and micro-sized pozzolanic materials together appears to have partially improved the imbalance in particle size.

When cured at a temperature of 45 °C, the initial and final setting time accelerated and the overall tendency was similar to the results obtained when curing was conducted at 20 °C. The fastest initial and final setting times of 72 and 92 min, respectively, were observed in the mix containing both nano- and micro-sized pozzolanic materials simultaneously. There was a reduction in overall setting time of all the mixes when cured at 45 °C. If strength increase is attributable to the densification of the microstructure alone without any influence of the pozzolanic reaction, then a predictable constant trend could have been established. In contrast, the finding that the setting times are indeed influenced by the curing temperature indicates that it is imperative that the hydration characteristics of the pozzolanic materials substituted as binders should be given serious consideration.

4.3. Compressive Strength Measurement Results

Figure 6 shows the compressive strength measurement results corresponding to the mixes with different pozzolanic binders and curing temperatures. For compressive strength measurement, the average value for six specimens was used. The measurement errors were within 5%. Strength measurements were summarized according to the contents of each mix and multiples of the setting time. The compressive strength improvement rate is expressed in the form of $y = A \cdot \ln(x) - B$ as a logarithmic function of time. Here, A varies depending on the compressive strength improvement rate. In the case of OPC, it attained the highest value of 17.857 at 10 °C curing temperature and followed a decreasing trend as the curing temperature increased; it dropped down to the level of 56.47% for 45 °C curing temperature. This trend is very similar to that evidenced in strength development corresponding to the curing conditions, which is typical in the case of cement paste. In the case of micro-silica, a tendency similar to that of OPC was observed. However, the compressive strength dropped down to the level of 89.51% for 45 °C curing temperature, thus registering a sharp difference in the extent of reduction in relation to the curing temperature. The mix containing nano-silica also exhibited a tendency similar to the aforementioned cases, but the strength improvement rate at lower temperature was high at 20.749. Particularly, in the mix substituted with both nano- and micro-silica together, the strength improvement rate and the initial strength were both high, and the highest value of 20.105 was observed for 20 °C curing temperature. The difference in strength improvement rate depending on the curing temperature was also found to be the smallest, as the level ranged from 91.08 to 93.3%. Based on the aforementioned results, it is evident that the use of pozzolanic materials improved the initial strength due to increased filling rate of the internal pores and the influence of the curing temperature declined because of the densification of the internal structure, which, in turn, reduced the impact of the external temperature. Micro-silica has average particle sizes in the range of 20 to 30 nm. It accelerated setting time in the same manner as the filling effect of nano-silica with a particle size of approximately 14.05 nm. Although the diameter of the average micro-silica particle is approximately twice as much as that of the average nano-silica particle, the volumes may differ by 9.73 times. It is quite evident from the aforementioned results that both micro-silica and nano-silica improved strength by generating hydrates through the pozzolanic reaction.

4.4. Activation Energy Measurement Results

Activation energy can be measured from the results of the regression analysis on the natural log value of the rate constant coefficient and the reciprocal of the absolute

temperature. Figure 7 shows the activation energy of the mixes containing OPC and pozzolanic binders. The activation energy values were calculated to be 58.62, 46.36, and 61.73 kJ/mol for the mixes containing OPC, micro-silica, and nano-silica, respectively. It is evident that the addition of micro-silica to the mix has caused the decrease in the minimum energy for activation, which, in turn, affected strength improvement. However, in the case of nano-silica, higher activation energy was measured in comparison to OPC. This can be attributed to the fact that nano-silica was significantly affected by the curing temperature in comparison to both OPC and micro-silica. While all siliceous materials are favorable for high-temperature curing [30–33], the compressive strength improvement rate of the nano-silica mix was the highest at low temperatures and it was measured to be similar to that of OPC at typical curing temperature. This is also attributable to the observation that compressive strength was significantly affected by curing temperature because the particles inside the microstructure were not dense and exhibited an imbalance due to the wide particle size difference between cement and nano-silica. In the case of the mix containing both micro-silica and nano-silica together, activation energy similar to that of the micro-silica mix was calculated without this effect. The activation energy was approximately 78.8% of that of OPC. Evidently, this activation energy evaluation reflects both the hydration reactions of cement and binders as well as the filling effect inside the microstructure. Hence, nano-CT imaging was performed to examine the pore structure inside the microstructure.

4.5. Microstructure (X-ray CT) Measurement Results

Images of the microstructure were captured using nano-CT equipment to evaluate the porosities of the specimens (Figure 8). Figure 9 shows the porosities of the silicate-based binder composites at the ages of 7 and 28 days. The microstructure analysis results established that the porosity of the specimens declined with time, i.e., porosity on day 28 is lower than that on day 7. OPC exhibited the highest total porosity, followed by the nano-silica mix, micro-silica mix, and the mix containing both nano-silica and micro-silica. The nano-silica mix showed the lowest porosity reduction rate between the ages of 7 and 28 days. Its porosity at 7 days was approximately 72.5% of that of OPC, but it was similar to that of OPC at 28 days (approximately 90.9%). In the case of micro-silica, however, the porosity sharply decreased, as it was approximately 39.9 and 33.1% of those of OPC at 7 and 28 days, respectively. The porosity further decreased in the specimen where both nano-silica and micro-silica were added.

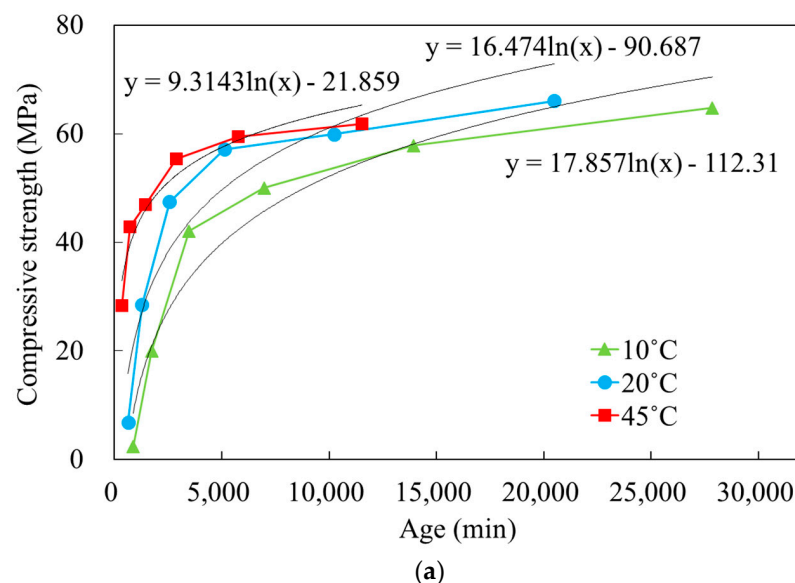


Figure 6. Cont.

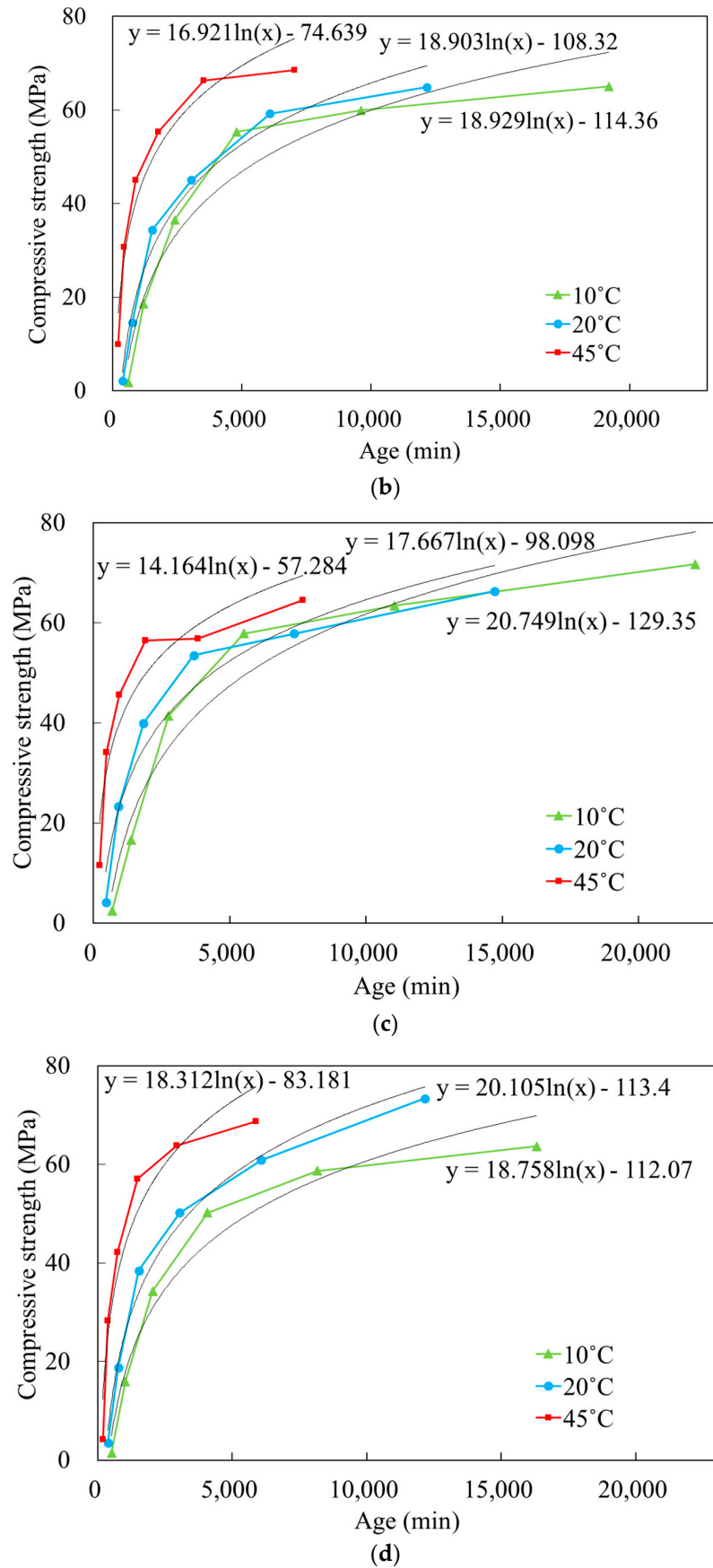


Figure 6. Compressive strengths of silicate-based binder composites. (a) OPC. (b) MS10. (c) NS1. (d) MS10NS1.

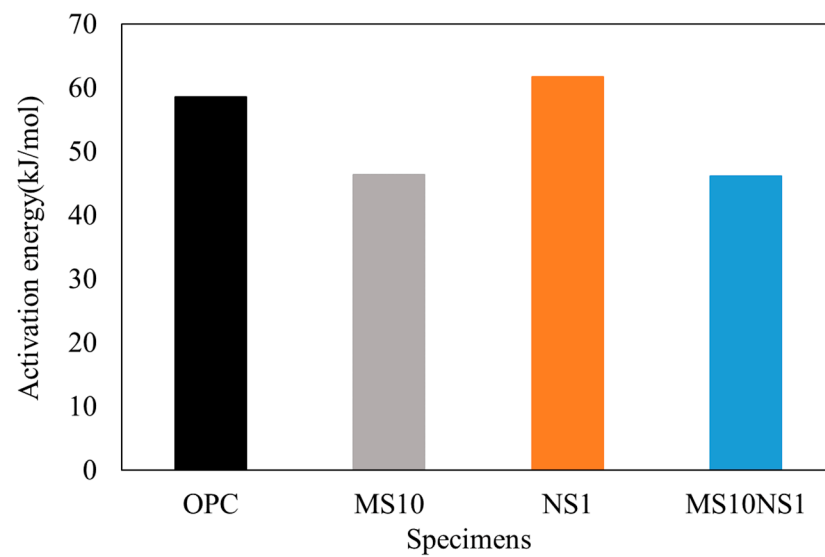


Figure 7. Activation energies of silicate-based binder composites.

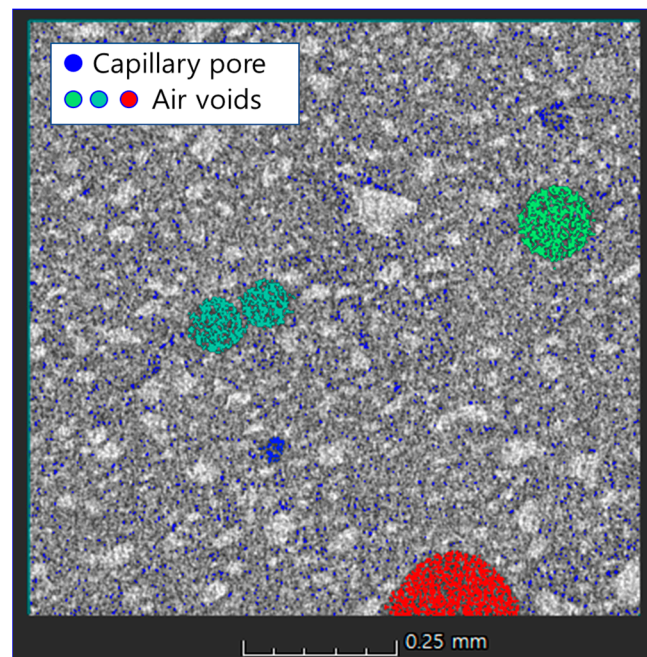


Figure 8. X-ray CT scan cross-sectional captured image of cement paste sample (NS1 specimens).

Similar to the activation energy experiment wherein the nano-silica mix required the highest energy, connected pores of size 100 nm or higher were present at the same level as that in OPC at 28 days in the nano-silica mix. However, in the specimen where micro-silica and nano-silica were added together, the extent of decrease in porosity was even higher. This indicates that the use of both nano-silica and micro-silica caused a balance in the distribution of particles, whereas the use of nano-silica alone had no significant filling effect among the cement particles owing to imbalance in the particle size distribution. Most likely, this interfered with the generation of hydrates on the surface of cement particles during hydration and had an adverse effect. At the beginning of the hydration reaction, the filling effect in the microstructure and the pozzolanic reaction resulted in reductions in porosity and setting time. However, the requirement of higher level of activation energy impedes the hydration reaction between nano-silica and cement in the long term, thereby decreasing the level of porosity reduction in the microstructure. If the particle size distribution is im-

balanced, the porosity within the microstructure is bound to increase [34]. A representative example of this is UHPC. Based on these observations, it can be summarized that, when silicate-based nanomaterials are considered for use, either the micro-sized pozzolanic materials should be applied together or special attention should be accorded to their particle size distribution.

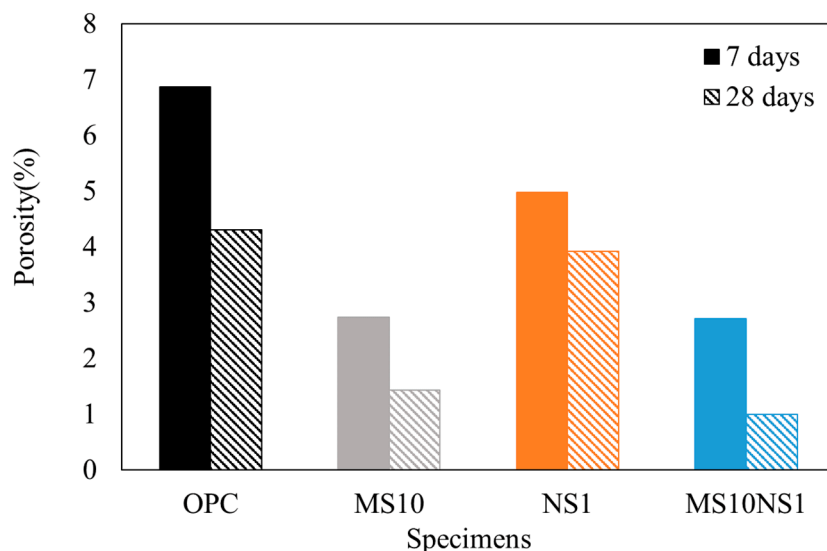


Figure 9. Porosities for silicate-based binder composites at different curing ages.

5. Conclusions

In this study, the setting time and activation energy of the mixes that used nano-silica and micro-silica as binders were measured and their mechanical properties were examined to investigate the effects of silicate-based nano- and micro-sized pozzolanic materials on the cement hydration reaction. Additionally, changes to the microstructure porosity caused by such effects were also examined, and the following conclusions can be drawn:

1. Because flowability decreases when silicate-based binders containing nanoparticles are added, attention needs to be paid to decisions on the addition of chemical admixtures as well as the water-to-cement ratio during mix design.
2. Both the initial and final setting times were reduced in mixes where silicate-based binders were added. In comparison to OPC, the addition of micro-silica has the largest setting acceleration effect. Nano-silica had a setting-promoting effect through a pozzolanic reaction even at a low content.
3. The compressive strength test results showed that the initial strength improvement rate was high when the silicate-based binders were used. Particularly, the effect was more profound under high-temperature curing conditions. The mix containing both nano-silica and micro-silica was impacted the most at pozzolanic reaction.
4. The highest activation energy was measured in the mix containing nano-silica. The mix containing micro-silica showed low activation energy (approximately 80% compared to OPC). When both nano-silica and micro-silica were added, the decrement increased.
5. Because the average particle size of cement is approximately 1400 times larger than that of nano-silica, evidently, the imbalance in particle size distribution had an adverse effect on both the strength improvement rate, which was not high, and the activation energy, which turned out to be high. This indicates that the particle size distribution plays an important role in the characteristics of the cement paste.
6. Porosity in the microstructure also showed a similar tendency. In the mix where nano-silica was used, the initial porosity significantly decreased compared to OPC. The porosity at the age of 28 days, however, was measured to be 90% of that of OPC. This indicates that nano-silica interferes with the hydration reaction of cement, thereby causing the porosity reduction in the microstructure.

7. The use of the silicate-based nano- and micro-sized pozzolanic materials influenced initial hydration positively by reducing the setting time and the porosity inside the microstructure, due to the internal pore-filling effect, thereby improving the compressive strength. Therefore, when silicate-based nano- and micro-sized pozzolanic materials are used, it is necessary to consider porosity of the conventional cementitious materials and their particle size distribution.

Therefore, when using nano- and micro-sized pozzolanic materials, the role of densification of the microstructure is important but, since it can be affected by the material's own characteristics, it is necessary to study reactivity through experiments such as activation energy.

Author Contributions: Methodology, W.-W.K.; Writing—original draft, W.-W.K.; Writing—review & editing, J.-H.M.; Supervision, J.-H.M. All authors have read and agreed to the published version of the manuscript.

Funding: Ministry of Land, Infrastructure, and Transport/Korea Agency for Infrastructure Technology Advancement (KAIA) (Grant No. 23NANO-C156177-04).

Data Availability Statement: Data are contained within the article.

Conflicts of Interest: The authors declare no conflict of interest.

References

1. Whatmore, R.W.; Corbett, J. Nanotechnology in the marketplace. *Comput. Control. J.* **1995**, *6*, 105–107.
2. Richard, P.; Cheyrezy, M. Composition of reactive powder concrete. *Cem. Concr. Res.* **1995**, *25*, 1501–1511. [[CrossRef](#)]
3. Zanni, H.; Cheyrezy, M.; Maret, V.; Philippot, S.; Nieto, P. Investigation of hydration and pozzolanic reaction in reactive powder concrete (RPC) using ^{29}Si NMR. *Cem. Concr. Res.* **1996**, *26*, 93–100. [[CrossRef](#)]
4. Goldman, A.; Bentur, A. The influence of micro-fillers on enhancement of concrete strength. *Cem. Concr. Res.* **1993**, *23*, 962–972. [[CrossRef](#)]
5. Li, H.; Xiao, H.-G.; Yuan, J.; Ou, J. Microstructure of cement mortar with nanoparticles. *Compos. Part B* **2004**, *35*, 185–189. [[CrossRef](#)]
6. Lee, N.K.; Koh, K.T.; Kim, M.O.; Ryu, G.S. Uncovering the role of micro silica in hydration of ultrahigh-performance concrete (UHPC). *Cem. Concr. Res.* **2017**, *104*, 68–79. [[CrossRef](#)]
7. Dong, S.; Wang, Y.; Ashour, A.; Han, B.; Ou, J. Nano/micro-structures and mechanical properties of ultrahigh-performance concrete incorporating graphene with different lateral sizes. *Compos. Part A App. Sci. Manuf.* **2020**, *137*, 106011. [[CrossRef](#)]
8. Yu, R.; Zhang, X.; Hu, Y.; Li, J.; Zhou, F.; Liu, K.; Zhang, J.; Wang, J.; Shui, Z. Development of a rapid hardening ultrahigh-performance concrete (R-UHPC): From macro properties to microstructure. *Constr. Build. Mater.* **2022**, *329*, 127188. [[CrossRef](#)]
9. Poppe, A.M.; Schutter, D.G. Analytical hydration model for filler rich binders in self-compacting concrete. *J. Adv. Concr. Tech.* **2006**, *4*, 259–266. [[CrossRef](#)]
10. Carino, N.J.; Knab, L.L.; Clifton, J.R. *NISTIR-4819 Applicability of the Maturity Method to High-Performance Concrete*; National Institute of Standards and Technology: Gaithersburg, MD, USA, 1992.
11. Adamu, M.; Ibrahim, Y.E.; Al-Atroush, M.E.; Alanazi, H. Mechanical properties and durability performance of concrete containing calcium carbide residue and nano silica. *Materials* **2021**, *14*, 6960. [[CrossRef](#)]
12. Wu, L.; Lu, Z.; Zhuang, C.; Chen, Y.; Hu, R. Mechanical properties of nano SiO_2 and carbon fiber reinforced concrete after exposure to high temperatures. *Materials* **2019**, *12*, 3773. [[CrossRef](#)] [[PubMed](#)]
13. Ye, Q.; Zhang, Z.; Kong, D.; Chen, R. Influence of nano- SiO_2 addition on properties of hardened cement paste as compared with silica fume. *Constr. Build. Mater.* **2005**, *21*, 539–545.
14. Yang, H.M.; Kwon, S.J.; Myung, N.V.; Singh, J.K.; Lee, H.S.; Mandal, S. Evaluation of strength development in concrete with ground granulated blast furnace slag using apparent activation energy. *Materials* **2020**, *13*, 442. [[CrossRef](#)] [[PubMed](#)]
15. Mun, J.S.; Yang, K.H.; Jeon, Y.S. Maturity-based model for concrete compressive strength with different supplementary cementitious materials. *J. Korea Inst. Struct. Maint. Insp.* **2014**, *18*, 082–089.
16. Zidi, Z.; Ltifi, M.; Zafar, I. Synthesis and attributes of nano- SiO_2 local metakaolin based-geopolymer. *J. Build. Eng.* **2021**, *33*, 101586. [[CrossRef](#)]
17. Lo, K.W.; Lin, K.L.; Cheng, T.W.; Chang, Y.M.; Lan, J.Y. Effect of nano- SiO_2 on the alkali-activated characteristics of spent catalyst metakaolin-based geopolymers. *Constr. Build. Mater.* **2017**, *143*, 455–463. [[CrossRef](#)]
18. Yang, L.Y.; Jia, Z.J.; Zhang, Y.M.; Dai, J.G. Effects of nano- TiO_2 on strength, shrinkage and microstructure of alkali activated slag pastes. *Cem. Concr. Compos.* **2015**, *57*, 1–7. [[CrossRef](#)]
19. Alomayri, T. Experimental study of the microstructural and mechanical properties of geopolymer paste with nano material (Al_2O_3). *J. Build. Eng.* **2019**, *25*, 100788. [[CrossRef](#)]

20. Zhang, C.; Khorshidi, H.; Najafi, E.; Ghasemi, M. Fresh, mechanical and microstructural properties of alkali-activated composites incorporating nanomaterials: A comprehensive review. *J. Clean. Prod.* **2023**, *15*, 135390. [[CrossRef](#)]
21. Kim, W.W.; Moon, J.H.; Baek, C.W.; Yang, K.H. Experimental study on the applicability of reactivity SiO₂ nano-materials as cement composites. *Korean Recycl. Constr. Resour. Inst.* **2021**, *9*, 529–536. (In Korean)
22. Mehta, P.K. History and status of performance tests for evaluation of the soundness of cements. In *Cement Standards Evolution and Trends*; ASTM International: West Conshohocken, PA, USA, 1978; STP357855.
23. Kabir, H.; Hooton, R.D.; Popoff, N.J. Evaluation of cement soundness using the ASTM C151 autoclave expansion test. *Cem. Concr. Res.* **2020**, *136*, 106159. [[CrossRef](#)]
24. ASTM C305; Standard Practice for Mechanical Mixing of Hydraulic Cement Pastes and Mortars of Plastic Consistency. American Society for Testing and Materials (ASTM). ASTM International: West Conshohocken, PA, USA, 2020.
25. *Korean Standard L5109*; Practice for Mechanical Mixing of Hydraulic Cement Pastes and Mortars of Plastic Consistency. Korean Standards Association (KSA): Seoul, Republic of Korea, 2017.
26. *Korean Standard L5111*; Flow Table for Use in Tests of Hydraulic Cement. Korean Standards Association (KSA): Seoul, Republic of Korea, 2022.
27. ASTM C191; Standard Test Methods for Time of Setting of Hydraulic Cement by Vicat Needle. American Society for Testing and Materials (ASTM). ASTM International: West Conshohocken, PA, USA, 2021.
28. ASTM C109; Standard Test Method for Compressive Strength of Hydraulic Cement Mortars (Using 2-in. or 50mm Cube Specimens). American Society for Testing and Materials (ASTM). ASTM International: West Conshohocken, PA, USA, 2020.
29. ASTM C1074; Standard Practice for Estimating Concrete Strength by Means of the Maturity Method. American Society for Testing and Materials (ASTM). ASTM International: West Conshohocken, PA, USA, 2019.
30. Short, N.; Page, C. Diffusion of chloride ions in hardened cement pastes. *Cem. Concr. Res.* **1981**, *11*, 395–406.
31. Park, C.; Jung, Y.S.; Seo, C.H. An experimental study on the characteristics of microporous structure formation by curing condition of cement blast furnace slag composite. *J. Archit. Inst. Korea Struct. Constr.* **2017**, *33*, 63–70. [[CrossRef](#)]
32. Liu, M.; Tan, H.; He, X. Effects of nano-SiO₂ on early strength and microstructure of steam-cured high volume fly ash cement system. *Constr. Build. Mater.* **2018**, *194*, 350–359. [[CrossRef](#)]
33. Nili, M.; Ehsani, A.; Shabani, K. Influence of nano-SiO₂ and microsilica on concrete performance. In Proceedings of the 2nd International Conference on Sustainable Construction Materials and Technologies, Ancona, Italy, 28–30 June 2010.
34. Wille, K.; Naaman, A.E.; Tawil, S.E.; Montesinos, G.J.P. Ultra-high performance concrete and fiber reinforced concrete: Achieving strength and ductility without heat curing. *Mater. Struct.* **2012**, *45*, 309–324. [[CrossRef](#)]

Disclaimer/Publisher’s Note: The statements, opinions and data contained in all publications are solely those of the individual author(s) and contributor(s) and not of MDPI and/or the editor(s). MDPI and/or the editor(s) disclaim responsibility for any injury to people or property resulting from any ideas, methods, instructions or products referred to in the content.